

A Search for Heavy Leptons at HERA

H1 Collaboration

Abstract:

A search for direct production of new leptons in the mass range from 10 GeV up to 225 GeV is presented by the H1 experiment at HERA. The data were obtained during 1993 and correspond to an integrated luminosity of 528 nb^{-1} . The search includes heavy lepton decays to final states $e(\nu)\gamma$ and $e(\nu)W$, $e(\nu)Z$ with the subsequent decay of the W and Z bosons into jets or lepton pairs. No evidence was found for the production of new massive electrons or neutrinos in any of the decay channels. Rejection limits for excited electrons and neutrinos are derived.

H1 Collaboration

T. Ahmed³, S. Aid¹³, V. Andreev²⁴, B. Andrieu²⁷, R.-D. Appuhn¹¹, M. Arpagaus³⁵,
A. Babaev²⁵, J. Baehr³⁴, J. Bán¹⁷, P. Baranov²⁴, E. Barrelet²⁸, W. Bartel¹¹, M. Barth⁴,
U. Bassler²⁸, H.P. Beck³⁶, H.-J. Behrend¹¹, A. Belousov²⁴, Ch. Berger¹, H. Bergstein¹,
G. Bernardi²⁸, R. Bernet³⁵, G. Bertrand-Coremans⁴, M. Besançon⁹, P. Biddulph²²,
J.C. Bizot²⁶, V. Blobel¹³, K. Borras⁸, F. Botterweck⁴, V. Boudry²⁷, A. Braemer¹⁴, F. Brasse¹¹,
W. Braunschweig¹, V. Brisson²⁶, D. Bruncko¹⁷, C. Brune¹⁵, R. Buchholz¹¹, L. Büngener¹³,
J. Bürger¹¹, F.W. Büsler¹³, A. Buniatian^{11,38}, S. Burke¹⁸, G. Buschhorn²⁵, A.J. Campbell¹¹,
T. Carli²⁵, F. Charles¹¹, D. Clarke⁵, A.B. Clegg¹⁸, M. Colombo⁸, J.G. Contreras⁸,
J.A. Coughlan⁵, A. Courau²⁶, Ch. Coutures⁹, G. Cozzika⁹, L. Criegee¹¹, D.G. Cussans⁵,
J. Cvach²⁹, S. Dagoret²⁸, J.B. Dainton¹⁹, M. Danilov²³, W.D. Dau¹⁶, K. Daum³³, M. David⁹,
E. Deffur¹¹, B. Delcourt²⁶, L. Del Buono²⁸, A. De Roeck¹¹, E.A. De Wolf⁴, P. Di Nezza³¹,
C. Dollfus³⁶, J.D. Dowell³, H.B. Dreis², J. Duboc²⁸, D. Düllmann¹³, O. Dünker¹³, H. Duhm¹²,
J. Ebert³³, T.R. Ebert¹⁹, G. Eckerlin¹¹, V. Efremenko²³, S. Egli³⁶, H. Ehrlichmann³⁴,
S. Eichenberger³⁶, R. Eichler³⁵, F. Eisele¹⁴, E. Eisenhandler²⁰, R.J. Ellison²², E. Elsen¹¹,
M. Erdmann¹⁴, E. Evrard⁴, L. Favart⁴, A. Fedotov²³, D. Feeken¹³, R. Felst¹¹, J. Feltesse⁹,
J. Ferencei¹⁵, F. Ferrarotto³¹, K. Flamm¹¹, M. Fleischer¹¹, M. Flieser²⁵, G. Flüge²,
A. Fomenko²⁴, B. Fominykh²³, M. Forbush⁷, J. Formánek³⁰, J.M. Foster²², G. Franke¹¹,
E. Fretwurst¹², E. Gabathuler¹⁹, K. Gabathuler³², K. Gamberdinger²⁵, J. Garvey³, J. Gayler¹¹,
M. Gebauer⁸, A. Gellrich¹³, H. Genzel¹, R. Gerhards¹¹, U. Goerlach¹¹, L. Goerlich⁶,
N. Gogitidze²⁴, M. Goldberg²⁸, D. Goldner⁸, B. Gonzalez-Pineiro²⁸, A.M. Goodall¹⁹,
I. Gorelov²³, P. Goritchev²³, C. Grab³⁵, H. Grässler², R. Grässler², T. Greenshaw¹⁹,
G. Grindhammer²⁵, A. Gruber²⁵, C. Gruber¹⁶, J. Haack³⁴, D. Haidt¹¹, L. Hajduk⁶,
O. Hamon²⁸, M. Hampel¹, E.M. Hanlon¹⁸, M. Hapke¹¹, W.J. Haynes⁵, J. Heatherington²⁰,
V. Hedberg²¹, G. Heinzlmann¹³, R.C.W. Henderson¹⁸, H. Henschel³⁴, R. Herma¹,
I. Herynek²⁹, M.F. Hess²⁵, W. Hildesheim¹², P. Hill⁵, K.H. Hiller³⁴, C.D. Hilton²², J. Hladký²⁹,
K.C. Hoeger²², M. Höppner⁸, R. Horisberger³², Ph. Huet⁴, H. Hufnagel¹⁴, M. Ibbotson²²,
H. Itterbeck¹, M.-A. Jabiol⁹, A. Jacholkowska²⁶, C. Jacobsson²¹, M. Jaffre²⁶, J. Janoth¹⁵,
T. Jansen¹¹, L. Jönsson²¹, K. Johannsen¹³, D.P. Johnson⁴, L. Johnson¹⁸, H. Jung¹¹,
P.I.P. Kalmus²⁰, D. Kant²⁰, R. Kaschowitz², P. Kassermann¹², U. Kathage¹⁶,
H.H. Kaufmann³⁴, S. Kazarian¹¹, I.R. Kenyon³, S. Kermiche²⁶, C. Keuker¹, C. Kiesling²⁵,
M. Klein³⁴, C. Kleinwort¹³, G. Knies¹¹, W. Ko⁷, T. Köhler¹, H. Kolanoski⁸, F. Kole⁷,
S.D. Kolya²², V. Korbelt¹¹, M. Korn⁸, P. Kostka³⁴, S.K. Kotelnikov²⁴, M.W. Krasny^{6,28},
H. Krehbiel¹¹, D. Krücker², U. Krüger¹¹, U. Krüner-Marquis¹¹, J.P. Kubenka²⁵, H. Küster²,
M. Kuhlen²⁵, T. Kurča¹⁷, J. Kurzhöfer⁸, B. Kuznik³³, D. Lacour²⁸, F. Lamarche²⁷, R. Lander⁷,
M.P.J. Landon²⁰, W. Lange³⁴, P. Lanius²⁵, J.F. Laporte⁹, A. Lebedev²⁴, C. Leverenz¹¹,
S. Levonian^{11,24}, Ch. Ley², A. Lindner⁸, G. Lindström¹², F. Linsel¹¹, J. Lipinski¹³, B. List¹¹,
P. Loch²⁶, H. Lohmander²¹, G.C. Lopez²⁰, D. Lüke^{8,11}, N. Magnussen³³, E. Malinowski²⁴,
S. Mani⁷, R. Maraček¹⁷, P. Marage⁴, R. Marshall²², J. Martens³³, R. Martin¹⁹, H.-U. Martyn¹,
J. Martyniak⁶, S. Masson², T. Mavroidis²⁰, S.J. Maxfield¹⁹, S.J. McMahon¹⁹, A. Mehta²²,
K. Meier¹⁵, D. Mercer²², T. Merz¹¹, C.A. Meyer³⁶, H. Meyer³³, J. Meyer¹¹, S. Mikocki⁶,
D. Milstead¹⁹, F. Moreau²⁷, J.V. Morris⁵, G. Müller¹¹, K. Müller³⁶, P. Murin¹⁷,
V. Nagovizin²³, R. Nahnhauser³⁴, B. Naroska¹³, Th. Naumann³⁴, P.R. Newman³, D. Newton¹⁸,
D. Neyret²⁸, H.K. Nguyen²⁸, F. Niebergall¹³, C. Niebuhr¹¹, R. Nisius¹, G. Nowak⁶,
G.W. Noyes³, M. Nyberg-Werther²¹, H. Oberlack²⁵, U. Obrock⁸, J.E. Olsson¹¹, A. Panitch⁴,
C. Pascaud²⁶, G.D. Patel¹⁹, E. Peppel¹¹, E. Perez⁹, J.P. Phillips²², Ch. Pichler¹², D. Pitzl³⁵,
G. Pope⁷, S. Prell¹¹, R. Prosi¹¹, G. Rädcl¹¹, F. Raupach¹, P. Reimer²⁹, S. Reinshagen¹¹,
P. Ribarics²⁵, V. Riech¹², J. Riedlberger³⁵, S. Riess¹³, M. Rietz², S.M. Robertson³,
P. Robmann³⁶, H.E. Roloff³⁴, R. Roosen⁴, K. Rosenbauer¹, A. Rostovtsev²³, F. Rouse⁷,
C. Royon⁹, K. Rüter²⁵, S. Rusakov²⁴, K. Rybicki⁶, R. Rylko²⁰, N. Sahlmann², E. Sanchez²⁵,
D.P.C. Sankey⁵, M. Savitsky²³, P. Schacht²⁵, S. Schiek¹¹, P. Schleper¹⁴, W. von Schlippe²⁰,

C. Schmidt¹¹, D. Schmidt³³, G. Schmidt¹³, A. Schöning¹¹, V. Schröder¹¹, E. Schuhmann²⁵, B. Schwab¹⁴, A. Schwind³⁴, U. Seehausen¹³, F. Sefkow¹¹, M. Seidel¹², R. Sell¹¹, A. Semenov²³, V. Shekelyan²³, I. Sheviakov²⁴, H. Shooshtari²⁵, L.N. Shtarkov²⁴, G. Siegmon¹⁶, U. Siewert¹⁶, Y. Sirois²⁷, I.O. Skillicorn¹⁰, P. Smirnov²⁴, J.R. Smith⁷, Y. Soloviev²⁴, H. Spitzer¹³, R. Starosta¹, M. Steenbock¹³, P. Steffen¹¹, R. Steinberg², B. Stella³¹, K. Stephens²², J. Stier¹¹, J. Stiewe¹⁵, U. Stösslein³⁴, J. Strachota²⁹, U. Straumann³⁶, W. Struczinski², J.P. Sutton³, S. Tapprogge¹⁵, R.E. Taylor^{37,26}, V. Tchernyshov²³, C. Thiebaux²⁷, G. Thompson²⁰, I. Tichomirov²³, P. Truöl³⁶, J. Turnau⁶, J. Tutas¹⁴, P. Uelkes², A. Usik²⁴, S. Valkár³⁰, A. Valkárová³⁰, C. Vallée²⁸, P. Van Esch⁴, P. Van Mechelen⁴, A. Vartapetian^{11,38}, Y. Vazdik²⁴, M. Vecko²⁹, P. Verrecchia⁹, G. Villet⁹, K. Wacker⁸, A. Wagener², I.W. Walker¹⁸, A. Walther⁸, G. Weber¹³, M. Weber¹¹, D. Wegener⁸, A. Wegner¹¹, H.P. Wellisch²⁵, L.R. West³, S. Willard⁷, M. Winde³⁴, G.-G. Winter¹¹, Th. Wolff³⁵, A.E. Wright²², E. Wunsch¹¹, N. Wulff¹¹, T.P. Yiou²⁸, J. Žáček³⁰, Z. Zhang²⁶, M. Zimmer¹¹, W. Zimmermann¹¹, F. Zomer²⁶, and K. Zuber¹⁵

¹ *I. Physikalisches Institut der RWTH, Aachen, Germany^a*

² *III. Physikalisches Institut der RWTH, Aachen, Germany^a*

³ *School of Physics and Space Research, University of Birmingham, Birmingham, UK^b*

⁴ *Inter-University Institute for High Energies ULB-VUB, Brussels; Universitaire Instellingen Antwerpen, Wilrijk, Belgium^c*

⁵ *Rutherford Appleton Laboratory, Chilton, Didcot, UK^b*

⁶ *Institute for Nuclear Physics, Cracow, Poland^d*

⁷ *Physics Department and IIRPA, University of California, Davis, California, USA^e*

⁸ *Institut für Physik, Universität Dortmund, Dortmund, Germany^a*

⁹ *CEA, DSM/DAPNIA, CE-SACLAY, Gif-sur-Yvette, France*

¹⁰ *Department of Physics and Astronomy, University of Glasgow, Glasgow, UK^b*

¹¹ *DESY, Hamburg, Germany^a*

¹² *I. Institut für Experimentalphysik, Universität Hamburg, Hamburg, Germany^a*

¹³ *II. Institut für Experimentalphysik, Universität Hamburg, Hamburg, Germany^a*

¹⁴ *Physikalisches Institut, Universität Heidelberg, Heidelberg, Germany^a*

¹⁵ *Institut für Hochenergiephysik, Universität Heidelberg, Heidelberg, Germany^a*

¹⁶ *Institut für Reine und Angewandte Kernphysik, Universität Kiel, Kiel, Germany^a*

¹⁷ *Institute of Experimental Physics, Slovak Academy of Sciences, Košice, Slovak Republic*

¹⁸ *School of Physics and Materials, University of Lancaster, Lancaster, UK^b*

¹⁹ *Department of Physics, University of Liverpool, Liverpool, UK^b*

²⁰ *Queen Mary and Westfield College, London, UK^b*

²¹ *Physics Department, University of Lund, Lund, Sweden^f*

²² *Physics Department, University of Manchester, Manchester, UK^b*

²³ *Institute for Theoretical and Experimental Physics, Moscow, Russia*

²⁴ *Lebedev Physical Institute, Moscow, Russia*

²⁵ *Max-Planck-Institut für Physik, München, Germany^a*

²⁶ *LAL, Université de Paris-Sud, IN2P3-CNRS, Orsay, France*

²⁷ *LPNHE, Ecole Polytechnique, IN2P3-CNRS, Palaiseau, France*

²⁸ *LPNHE, Universités Paris VI and VII, IN2P3-CNRS, Paris, France*

²⁹ *Institute of Physics, Czech Academy of Sciences, Praha, Czech Republic^g*

³⁰ *Nuclear Center, Charles University, Praha, Czech Republic^g*

³¹ *INFN Roma and Dipartimento di Fisica, Università "La Sapienza", Roma, Italy*

³² *Paul Scherrer Institut, Villigen, Switzerland*

³³ *Fachbereich Physik, Bergische Universität Gesamthochschule Wuppertal, Wuppertal, Germany^a*

³⁴ *DESY, Institut für Hochenergiephysik, Zeuthen, Germany^a*

³⁵ *Institut für Teilchenphysik, ETH, Zürich, Switzerland^h*

³⁶ *Physik-Institut der Universität Zürich, Zürich, Switzerland^h*

³⁷ *Stanford Linear Accelerator Center, Stanford California, USA*

³⁸ *Visitor from Yerevan Phys.Inst., Armenia*

^a *Supported by the Bundesministerium für Forschung und Technologie, FRG under contract numbers 6AC17P, 6AC47P, 6DO57I, 6HH17P, 6HH27I, 6HD17I, 6HD27I, 6KI17P, 6MP17I, and 6WT87P*

^b *Supported by the UK Science and Engineering Research Council*

^c *Supported by FNRS-NFWO, IISN-IKW*

^d *Supported by the Polish State Committee for Scientific Research, grant No. 204209101*

^e *Supported in part by USDOE grant DE F603 91ER40674*

^f *Supported by the Swedish Natural Science Research Council*

^g *Supported by GA ĆR, grant no. 202/93/2423 and by GA AV ĆR, grant no. 19095*

^h *Supported by the Swiss National Science Foundation*

1 Introduction

At the present time, there is no clear experimental evidence for particle physics phenomena beyond the Standard Model (SM). The discovery of new heavy particle states would change this completely. A search for such particles has thus high priority at any new collider.

At the electron(e)-proton(p) collider HERA new heavy leptons could be produced as single intermediate states formed between the incoming electron and a gauge boson radiated off the proton. Particular examples of heavy leptons are excited electrons (e^*) and excited neutrinos (ν^*), which are a natural ingredient of composite models [1]. If found, they would constitute a proof for the existence of substructure in the fermion sector. In any case most extensions of the SM predict heavy particles. Right handed neutrinos [2] are another example of new heavy leptons which can be produced through charged current processes in ep scattering experiments. They appear, e.g., in unified theories based on the group $SO(10)$, in left-right symmetric theories, and in models with mirror fermions [3].

The search for heavy leptons at HERA has some advantages compared to current e^+e^- or $p\bar{p}$ machines. Larger masses are accessible for single heavy lepton production by virtue of the available energy compared with e^+e^- . In addition, incident leptons are present at HERA, lacking in $p\bar{p}$ colliders, and a violation of lepton number conservation in the decays of some heavy neutrinos could be discovered by detecting the resulting positively charged lepton.

Generally the ep cross section for the production of a heavy state L decaying into a specific final state with a branching ratio \mathcal{B} is given by

$$\sigma(e + p \rightarrow L + X) = \frac{4\pi^2}{s} (2J + 1) \frac{\Gamma}{M} \mathcal{B} f_{i/p}(M^2/s),$$

where J , M are the angular momentum and the mass of L , and \sqrt{s} is the centre of mass energy. This equation is valid in the narrow-width approximation and to lowest order (Born term). Here, $f_{i/p}(x) dx$ is the number of gauge bosons with momentum fraction x radiated off the proton. The widths Γ and the branching ratios \mathcal{B} depend on specific models for the coupling to these new particles.

In this paper we present a search for the production of new heavy leptons based on an integrated luminosity of $\mathcal{L} = 528 \pm 27 \text{ nb}^{-1}$ collected during 1993 at $\sqrt{s} = 296 \text{ GeV}$. First results with 1992 data (\mathcal{L} about 25 nb^{-1}) can be found elsewhere [5, 6].

2 Experimental Method

Heavy charged leptons would be produced dominantly by the exchange of low- Q^2 photons whereas heavy neutral leptons would be formed in a wider range of Q^2 through W boson exchange. Here, $-Q^2$ is the four-momentum squared of the gauge boson. The current maximum available centre of mass energy for the direct production of states L at HERA is 296 GeV. This allows the exploration of a mass range where L may decay via a heavy gauge boson (W or Z). If L is the lightest new lepton produced, it may decay into $l\gamma$, lZ , or lW where l stands for e or ν , respectively. The heavy gauge boson from the L decay will itself decay either into a quark(q)-antiquark(\bar{q}') pair, giving two final state jets, or into a lepton pair. Generally these decay products will have high transverse energies, E_t , and will reconstruct to the mass of the W or Z . An excess of events around these masses is a good signature for the production and decay of new states.

As far as possible, we have carried out the search for new heavy leptons in a model independent way. The ingredients of our analysis methods to investigate the different final states are:

searches for large E_t isolated electromagnetic (e.m.) clusters (localized energy deposit), large missing transverse energy, E_t^{miss} , and pairs of jets with high transverse energy. The analysis is based on the following combinations of these signatures:

1. Two isolated e.m. clusters, exclusively,
2. Two or more isolated e.m. clusters, inclusively, or one or more isolated e.m. clusters and large missing transverse energy,
3. Two or more jets with or without additional e.m. clusters.

The association of these search methods with specific decay modes are shown in Table 1.

Final State	Decay	Search Methods
$L \rightarrow e \gamma$	$e \gamma$	1 / 2
$\rightarrow e Z$	$Z \rightarrow e e / \nu \bar{\nu} / q \bar{q}'$	2 / 2 / 3
$\rightarrow \nu W$	$W \rightarrow e \nu / q \bar{q}'$	2 / 3
$\rightarrow \nu \gamma$	$\nu \gamma$	2
$\rightarrow \nu Z$	$Z \rightarrow e e / q \bar{q}'$	2 / 3
$\rightarrow e W$	$W \rightarrow e \nu / q \bar{q}'$	2 / 3

Table 1: *Decay modes of heavy leptons L considered in this analysis.*

Final states with only leptons and/or photons have a clean signature and a high detection efficiency. W or Z boson decays to $q \bar{q}'$ pairs are more difficult to detect and have comparatively more background.

Several background processes contribute to the various heavy lepton decay channels. In most cases the background arises from standard physics and is concentrated at low invariant masses ($\lesssim 60$ GeV). The events with low invariant mass systems constitute a good control sample for our search methods of high mass heavy leptons. Hence we select the events in a mass region starting at 10 GeV for all the different final states and compare our data with the prediction from standard physics processes. If agreement is found at low masses, we take the expectation at higher masses to be the background estimator, B , of the number of measured events, N . In absence of any signal, upper limits on couplings can be determined from N and B with a confidence level (CL) taking into account detection efficiencies and luminosity.

3 Experimental Set-up

A detailed description of the H1 detector can be found elsewhere [7]. Here we describe briefly the components which are relevant for this analysis. The interaction region is surrounded by a drift and proportional chamber tracking system, split into central barrel and forward parts and covering the angular range $7^\circ \leq \theta \leq 176^\circ$ ¹. The tracking system is placed inside a finely segmented liquid argon (LAr) calorimeter covering the range $4^\circ \leq \theta \leq 153^\circ$. The electromagnetic section, between 20 and 30 radiation lengths (X_0) deep, is used to identify electrons and photons. Hadrons also deposit energy in the outer layer (hadronic section) of the LAr calorimeter. The total thickness of the LAr components varies between 4.5 and 8 interaction lengths. For the LAr calorimeter energy resolutions of $\sigma(E)/E \simeq 12\%/\sqrt{E(\text{GeV})} \oplus 1\%$ for electrons and photons and

¹The forward direction (positive z -coordinate) from which the polar angle, θ , is measured is the incident proton beam direction.

$\sigma(E)/E \simeq 50 \text{ \%}/\sqrt{E(\text{GeV})} \oplus 2\%$ for hadrons have been obtained in test beam measurements. A 22 X_0 deep lead-scintillator e.m. calorimeter (BEMC) is located in the backward region ($151^\circ \leq \theta \leq 176^\circ$) of the H1 detector. The resolution is determined to be $\sigma(E)/E \simeq 10 \text{ \%}/\sqrt{E(\text{GeV})} \oplus 2\%$.

The tracking system and calorimeters are surrounded by a superconducting solenoid producing a uniform field of 1.15 T in the z -direction. The luminosity detectors, which measure the Bethe-Heitler reaction $ep \rightarrow e\gamma p$ and electrons from photoproduction processes, are placed at the positions $z = -33$ m (electron tagger) and at $z = -103$ m (photon tagger), with respect to the nominal interaction point.

4 Event Selection

4.1 Exclusive Electromagnetic Cluster Analysis

Events with two e.m. clusters only (see Table 1, search method 1) are candidates for charged heavy lepton decays, but also for the Wide-Angle Bremsstrahlung (WAB) background process $ep \rightarrow e\gamma p(X)$ with a well separated $e\gamma$ pair. Most of the WAB events are expected to have an $e\gamma$ system of low invariant mass ($\lesssim 20$ GeV) with high momentum in the direction of the incoming electron. Hence the outgoing electron and photon can be detected in the backward part of the calorimeters.

In most cases the hadronic system, $p(X)$, has a small transverse momentum and escapes detection. For elastic WAB events the final hadronic state consists of only a proton, while for the quasielastic and inelastic process the proton fragments. By our definition, the latter two processes are separated by regions in Q^2 , where for $Q^2 < 5 \text{ GeV}^2$ the process is called quasielastic, else it is inelastic.

The first step is the selection of events with two isolated e.m. clusters only, which are expected to be dominated by the background of elastic and quasielastic WAB processes. The cuts to select $e\gamma$ pairs are shown in Table 2 and define search method 1.

In total an accumulated luminosity of 528 nb^{-1} was analysed in this part. The events are required to have satisfied the BEMC or LAr energy triggers. The trigger efficiency for e.m. clusters with energies above 20 GeV in the BEMC and LAr is $\approx 100\%$. This was checked by studying deep inelastic scattering (DIS) electrons in the BEMC and in the LAr calorimeter and by using the e.m. showers produced by photons radiated off cosmic or beam halo muons.

We define an e.m. cluster to have at least 90 % of its energy deposited in the e.m. part of the calorimeters and to be isolated, based on a geometric cone about the e.m. cluster in terms of azimuthal angle ($\Delta\phi$) and pseudorapidity ($\Delta\eta$) differences with respect to the cluster centre. If less than 10% additional energy is within $R = \sqrt{\Delta\phi^2 + \Delta\eta^2} < 0.5$, the cluster is defined as isolated. Requirement 2 takes into account that for most elastic and quasielastic WAB events at low $e\gamma$ masses the summed energy of the two clusters is given by the energy, E , of the initial electron. Requirement 3 rejects events with other particles in the final state, where E_{total} is the energy deposit in the LAr and BEMC. Requirements 4 and 5 rely on the fact that for exclusive $L (\rightarrow e\gamma)$ production as well as for the elastic and quasielastic WAB background the kinematics of the process is overconstrained. The same physical quantity, e.g. the energy E_i of the outgoing electron or photon, or the mass m of the $e\gamma$ system, can be determined by two methods. First, the measured four vectors with the energies E_e and E_γ of the outgoing electron and photon are used to calculate m and second, only the polar angles θ_e, θ_γ are used to calculate $m^2(\theta_e, \theta_\gamma) = 4E^2(1 + \beta)/(1 - \beta)$, with $\beta = \sin(\theta_e + \theta_\gamma)/(\sin\theta_e + \sin\theta_\gamma)$ and similarly

Search method 1

1. ≥ 2 isolated e.m. clusters $E_i \geq 2$ GeV for $i = e, \gamma$
 2. $E_e + E_\gamma \geq 20$ GeV
 3. $E_{total} - E_e - E_\gamma < 5$ GeV
 4. $|m(\theta_e, \theta_\gamma) - m| < 2m$
 5. $|E_i(\theta_e, \theta_\gamma) - E_i| < E_i$
 6. $10^\circ < \theta_e < 160^\circ$ or $10^\circ < \theta_\gamma < 160^\circ$
 7. $20 \text{ GeV} < (E - p_z)_{total} < 80 \text{ GeV}$
 8. $m > 10$ GeV
 9. Visual scan
-
-

Table 2: *Selection requirements for elastic and quasielastic WAB events. Here m is the invariant mass of the $e\gamma$ system. The other quantities are explained in the text. If more than two isolated e.m. clusters are found, the two clusters fulfilling requirements 1 and 2 with the largest polar angles θ_i are used.*

$E_{e,\gamma}(\theta_e, \theta_\gamma) = 2E\beta/(1 - \beta)\sin\theta_{\gamma,e}/\sin(\theta_e + \theta_\gamma)$. Requirements 6 and 7 suppress background from DIS and γp events, respectively.

The 288 events above $m = 10$ GeV are visually scanned and events which have tracks uncorrelated with the e.m. clusters (82 events) are rejected. These events are not due to WAB processes as was checked by scanning WAB Monte Carlo events. In addition cosmic (59 events) and beam halo muons (62 events), which can have complicated topologies, are identified and removed at this stage. The remaining 85 events are compared to the WAB event simulation [8] which predicts 86 events above $m = 10$ GeV. The generated events, corresponding to a luminosity of 6 pb^{-1} , are fed into the H1 detector simulation program and are subject to the same reconstruction and analysis chain as the real data. The absolute number and the shapes of the distributions for the energies and angles of the e.m. clusters (not shown) as well as the $e\gamma$ mass spectrum (Figure 1) are reproduced well by the WAB simulation. Applying the Kolmogorov-Smirnov test the probability is 28% that both follow the same distribution. The highest measured mass is at 45 GeV. In total 0.6 events are expected from the WAB process for masses above 60 GeV.

4.2 Inclusive Electromagnetic Cluster Analysis

Candidates for more general event topologies from heavy lepton decays with one or more e.m. clusters as well as other particles in the final state must fulfill the selection criteria shown in Table 3, defining search method 2. The analysis is based on an integrated luminosity of 434 nb^{-1} , because more stringent data quality criteria are applied. The same triggers are used as in the previous analysis.

The selections in Table 3 are motivated by Monte Carlo studies and give a high signal detection efficiency whilst rejecting wrongly identified events like those from cosmic muons. 13 events remain after all requirements. The final classification is done visually. Three inelastic WAB events with an expectation of 2.1 are found with invariant masses of the $e\gamma$ system at 26 GeV, 38 GeV, and 57 GeV. The number of DIS candidates (10 events) in this sample is compared with the LEPTO Monte Carlo event simulation [9] which predicts 11 events in total. Four of the DIS events have an $E_t^{miss} > 12$ GeV. Under the assumption that a neutrino escapes detection, the invariant mass of the heavy electron and the heavy neutrino can be calculated. All masses are below 50 GeV and therefore these events are not considered to be candidates for heavy leptons decaying into the W or Z boson.

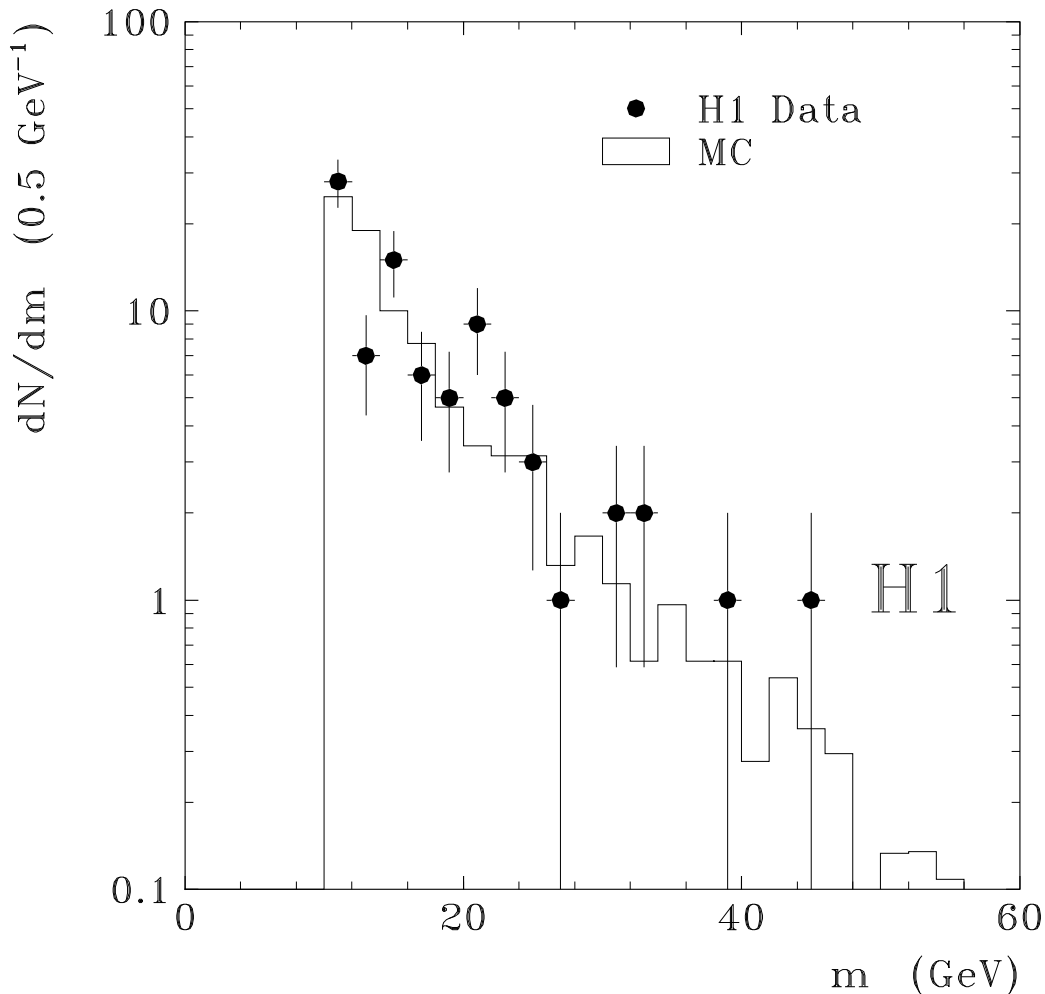


Figure 1: *Mass spectrum of the selected $e\gamma$ pairs above 10 GeV. The histogram shows the absolute prediction based on the WAB Monte Carlo simulation.*

Search method 2

1. ≥ 2 isolated e.m. clusters, $E_{t1} > 20$ GeV and $E_{t2} > 12$ GeV or
 ≥ 1 isolated e.m. cluster with $E_{t1} > 20$ GeV and $E_t^{miss} > 12$ GeV
 2. Cosmic and beam halo muon-filter
 3. Visual classification
-
-

Table 3: *Selection criteria of heavy lepton states. E_{t1} and E_{t2} are the transverse energies of the first and second cluster.*

In summary, after imposing the Table 3 selection requirements, no candidates are left with a mass above 60 GeV in final states which include e.m. clusters.

4.3 Jet Analysis

Events with two or more jets with a high invariant mass in the final state are candidates for decays of the heavy gauge bosons W and Z . Background is to be expected from photoproduction processes. The requirement for detecting two or more jets includes both the modes with an additional e or ν and also ensures that the detection efficiency remains high for new heavy

leptons just above the W or Z mass, where the electron is difficult to detect or E_t^{miss} is small. The subsequent cuts for the data selection with this final state topology are given in Table 4, defining search method 3.

This part of the analysis is based on an integrated luminosity of 320 nb^{-1} . For this luminosity the electron tagger could be used to control the background from photoproduction by identifying the tagged electron in the extreme backward direction.

Search method 3

-
-
1. ≥ 2 jets, $E_{ti} > 8 \text{ GeV}$, with $i = 1, 2$
 2. $\Delta\theta > 60^\circ$ or $m_{12} > 50 \text{ GeV}$
 3. Requirements on tracks
 4. $E_{tag} > 7 \text{ GeV}$ (set 1) or
 5. $E_{tag} \leq 7 \text{ GeV}$ (set 2)
 - 5.1 reject events with an electron: (set 2a)
 - 5.2 select events with an electron: (set 2b)
 - $\theta_e < 160^\circ$
 6. Visual verification
-
-

Table 4: *Selection criteria for the jet analysis. If more than two jets are found, the two jets with highest transverse energies E_{ti} are used. E_{tag} is the energy deposited in the electron tagger. Electrons are defined by $E_e > 10 \text{ GeV}$ and $\theta_e > 10^\circ$ (see also text).*

For the definition of the jets we use a cone algorithm with radius $R = 1$ in the η - ϕ -plane according to the Snowmass approach [10]. The opening angle $\Delta\theta$ between the jets from W or Z decays is in general large. For low invariant masses of the two jets ($m_{12} < 50 \text{ GeV}$) the requirement $\Delta\theta > 60^\circ$ gives a clean sample of candidate events, since the main background contribution from beam (p)-gas interaction is at small angular separation. For larger two jet masses, however, the $\Delta\theta$ cut is not applied because for new, very heavy ($\gtrsim 150 \text{ GeV}$) leptons decaying into massive gauge bosons, the W or Z is strongly boosted in the direction of the incident proton and small angles between the two jets become possible. For further suppression of beam-gas or beam-wall events we demand at least five tracks with $p_t > 0.2 \text{ GeV}$ in the central track chambers or less than 40 tracks without p_t requirement. No candidates from heavy lepton decays are expected with electrons above $\theta_e = 160^\circ$, where most of the background from DIS is anticipated.

We distinguish between events depositing more than 7 GeV energy in the electron luminosity detector (tagged events, set 1) and events where no electron is detected (untagged sample, set 2). Set 1 consists of photoproduction events, which are obviously *not* candidates for new heavy lepton production. This is a good control sample for the data without an electron tag (set 2) which are expected to contain mainly photoproduction and DIS events.

The events of set 1 have to be triggered by the electron tagger. In the untagged sample (set 2) and for invariant masses of the two jets above 60 GeV, events are required to be triggered either by the central tracking system or by the LAr calorimeter. For lower masses only triggers of the central tracker are required. The track-trigger efficiency for set 2 is determined from photoproduction data (set 1) monitored by the electron tagger, and the LAr trigger efficiency is calculated using the central track triggers as monitor. Both efficiencies are folded into the event simulation.

We compare our data with predictions based on the Monte Carlo generator PYTHIA [11] and take into account resolved and direct photoproduction of light and heavy quarks. The Lund

string model [12] is used for fragmentation and decay. The generated events with simulated H1 detector response, including the triggers, are reconstructed exactly the same way as real data.

First the tagged data sample $ep \rightarrow e_{tag} X$ (set 1) is compared with the photoproduction Monte Carlo simulation. With the cuts chosen, we find good agreement between the data and the expectation for the absolute number of events and the shapes of various distributions, e.g. the energy in the electron tagger, the transverse energies, the pseudorapidities, and the invariant mass of the jets. Next the sample with no electron detected in the final state, defined as set 2a in Table 4, is considered. Good agreement of the z -vertex distribution (mostly within ± 20 cm) is found between data and Monte Carlo expectation, using a vertex simulation based on data from DIS events, indicating that the beam-gas background contamination in the event sample is negligible. The distributions of jet transverse energies, E_{ti} , and pseudorapidities, in the 823 events of set 2a agree well with the photoproduction event simulation which predicts 802 events. Most of the events have jets at low E_{ti} as expected from photoproduction processes, extending up to 42 GeV, the region where decay products of heavy leptons might be found. The jet pseudorapidities vary between -2 and 2.5 .

Figure 2 displays the invariant mass spectrum of the two jets for events of set 2a, together with the expectation. These event topologies cover the decay modes $\nu q \bar{q}'$ and $e q \bar{q}'$ where the electron is not observed (see Table 1). The distributions agree both in shape and absolute normalization. Applying the Kolmogorov-Smirnov test in the mass range above 25 GeV the probability that both follow the same distribution is 32%. Due to our jet-jet mass resolution of about 10 GeV, candidates of W or Z decays are expected at measured invariant masses above 60 GeV. For events with large missing E_t (neutrino in the final state), the effective mass can still be calculated, using the missing transverse energy E_t^{miss} and $(E - p_z)_{total}$.

A spectacular two jet event with a reconstructed mass of 80 GeV is shown in Figure 3. The event conserves transverse momentum and is hence a candidate for W decay. The number of expected events from electroproduction of W bosons is around 0.3, according to the Monte Carlo generator EPEWAX [13].

With an additional requirement of at least two jets with $E_{ti} > 15$ GeV, designed to further optimise signal to background ratio, the number of events with invariant masses of the two jets above 60 GeV is 28 and the expectation from PYTHIA is 34. For masses above 80 GeV we observe 11 events where 5 are expected, corresponding to a probability of 5.8% taking into account the uncertainty of the expectation. The highest invariant mass found is at 101 GeV. We conclude that there is no evidence of any new heavy lepton signal in the whole mass interval.

Finally, we search for topologies with an extra electron (set 2b), covering the decay modes $e q \bar{q}'$. For high invariant masses of e +jets the electron requirement gives an additional constraint and ensures a better background suppression. The natural background in these channels comes from DIS events. After all selection requirements have been applied, one event with the topology e +jets remains, compatible with the expectation, and it has a reconstructed e +jets mass of 117 GeV.

In summary, after imposing selection requirements for the presence of heavy gauge bosons, no excess of events is found in any of the channels under study. Where candidates still survive the cuts, their number is compatible with expectations from the specific background processes.

5 Efficiency using a Specific Model

During the search for new heavy leptons no specific model has been assumed in order to be as sensitive as possible to a wide range of new particle states. To calculate limits on cross sections and couplings specific assumptions are required.

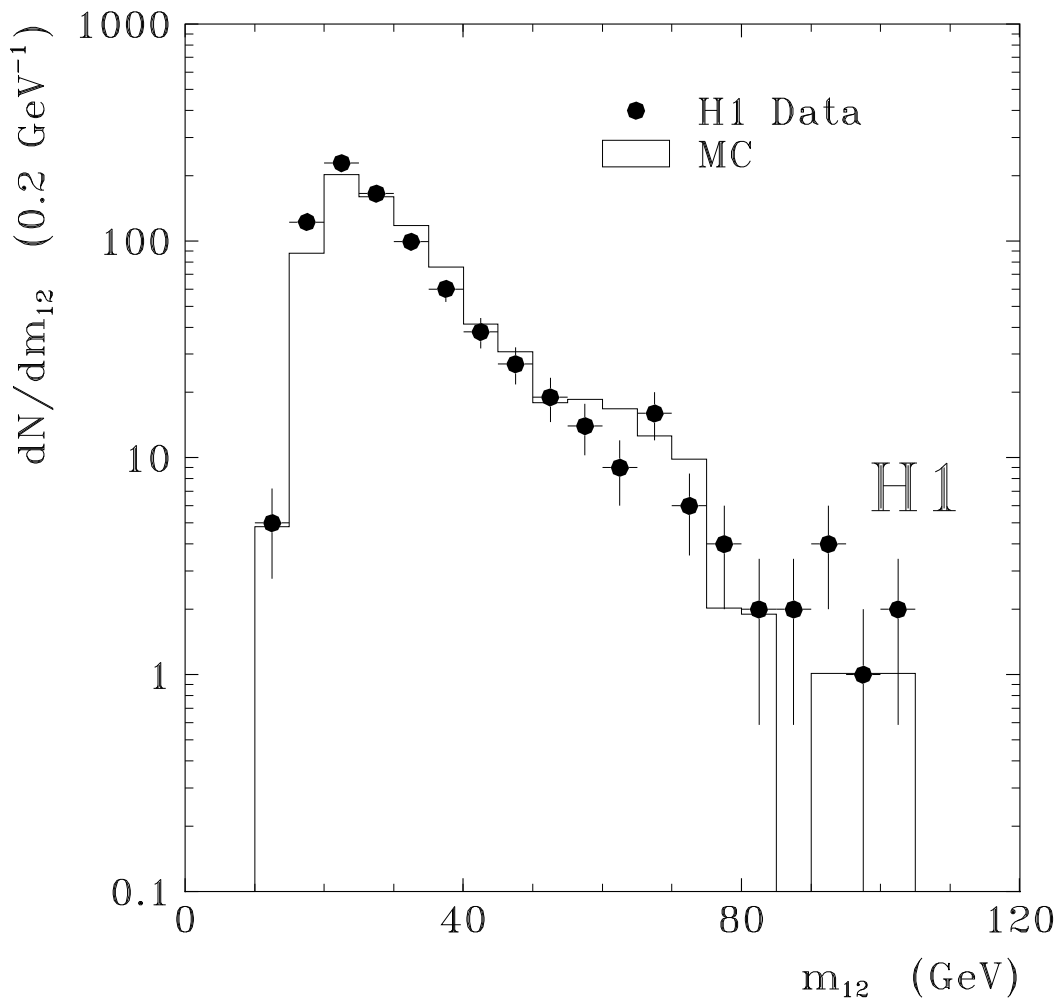


Figure 2: *Jet-jet mass spectrum above 10 GeV for final states with jets. The histogram shows the absolute prediction for photoproduction based on the PYTHIA Monte Carlo simulation corresponding to an integrated luminosity of 300 nb^{-1} .*

The theory for production of excited lepton states has been discussed extensively in the literature [14]. Here we use a model based on an effective $SU(2) \otimes U(1)$ invariant Lagrangian [15] for spin 1/2 excited states. In this model the magnetic transition couplings of an ordinary lepton (l) and an excited lepton (l^*) to a vector boson (V) with four momentum q are given by $-i \frac{e}{\Lambda} \sigma_{\mu\nu} q^\nu (1 - \gamma_5) c_{Vl^*l}$. Here, e is the electric charge, Λ is the compositeness scale, and c_{Vl^*l} are different coupling constants. In ep collisions the production of the excited leptons depends mainly on the couplings $c_{\gamma e^*e}$ and $c_{W\nu^*e}$ while for the decay of the excited states the other couplings have to be considered, too. The width Γ is approximately given by $\Gamma = \alpha M^3 c_{Vl^*l}^2 / \Lambda^2$. The branching ratios, calculated in refs. [4, 16], are *a priori* unknown because they depend on the unknown couplings c_{Vl^*l} .

For detailed studies the Monte Carlo event generator COMPOS [17] is used, which is based on the cross section calculated in ref. [15]. We employ the Lund string model for fragmentation and decays and all the results presented here have been obtained using the MRS D- parametrisation of the parton densities. The generated events are passed through the full H1 detector simulation and are reconstructed like real data. The total efficiency for a new excited lepton to survive the selection steps is then derived from this Monte Carlo simulation including also the trigger efficiencies. These total detection efficiencies are shown in Figure 4 for the different final states as a function of the mass of the heavy lepton for values above 75 GeV. The average detection efficiency for e^* events with masses between 25 GeV and 75 GeV is 60%. For channels with electrons and photons the efficiencies are between 60% and 95% whilst for final states with jets

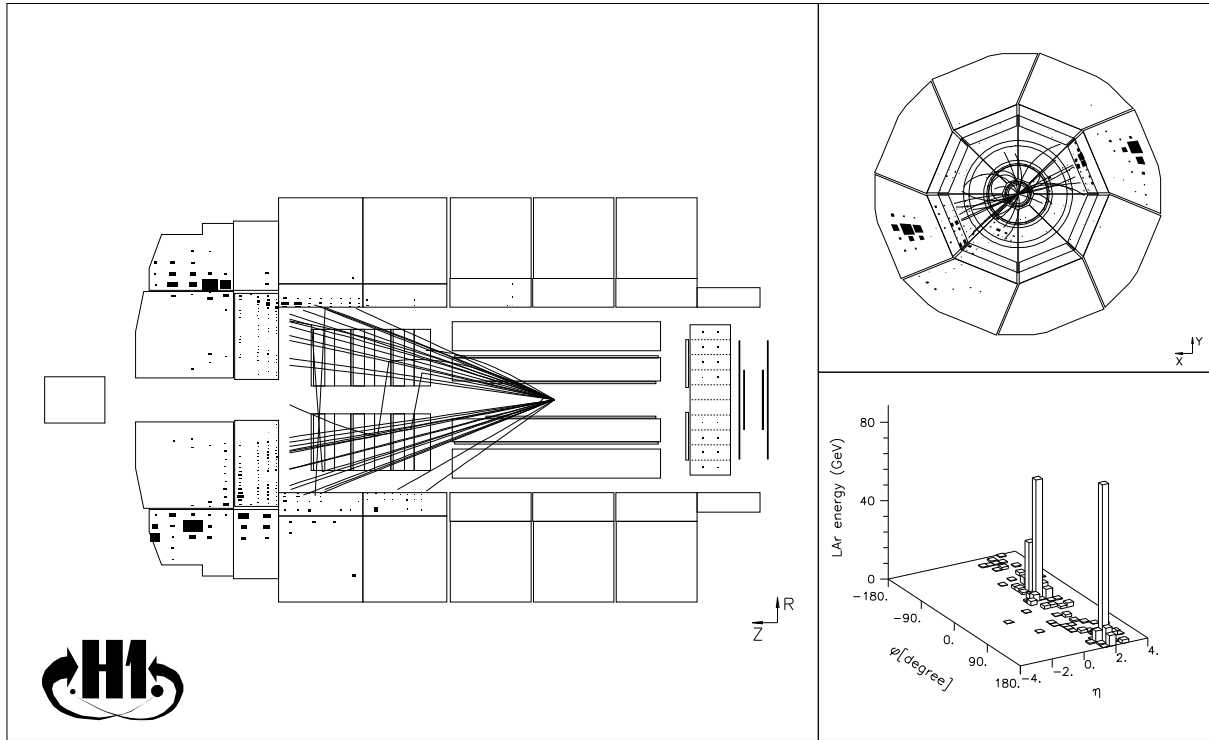


Figure 3: A two jet event in two projections of the H1 apparatus and the energy flow as measured in the calorimeter. The two jets have transverse energies of 42 GeV and 38 GeV. The invariant mass is determined to be 80 GeV.

the typical efficiencies are around 50%.

The rejection limits are derived by adapting the procedure recommended by the Particle Data Group [18]. In the channel $e^* \rightarrow e\gamma$ for masses below 75 GeV a luminosity of 528 nb^{-1} is used. For masses above 75 GeV and for all other channels without jets the relevant value is 434 nb^{-1} . For final states with jets a luminosity corresponding to 320 nb^{-1} is analysed. The uncertainties for calculating limits are due to the errors in the luminosity (5%), knowledge of the total efficiency (7%), the parton densities (6%), and the background estimator B ($\leq 17\%$). The errors on the total efficiencies are determined by varying the thresholds of our main selection criteria within reasonable bounds. The dependence on the parton density functions has been studied by employing various parametrisations. We estimate that the combination of these uncertainties for various decay channels yields an effective 7% uncertainty on the values of the coupling limits. Possible dependencies of the limits on the hadronisation model employed have been neglected.

6 Results

Using only the accumulated luminosity and the computed efficiencies, cross sections above $\mathcal{O}(10 \text{ pb})$ for the production of new heavy leptons are ruled out with 95% CL, depending on the decay channel. These limits are almost independent of the nature of the heavy state.

The experiment can set limits on the product of the coupling constant $c_{\nu_l^* l}$ with the square root of the branching ratio \mathcal{B} of the excited leptons divided by the compositeness scale parameter Λ . The 95% CL upper limits are shown in Figures 5 and 6 for each of the three different

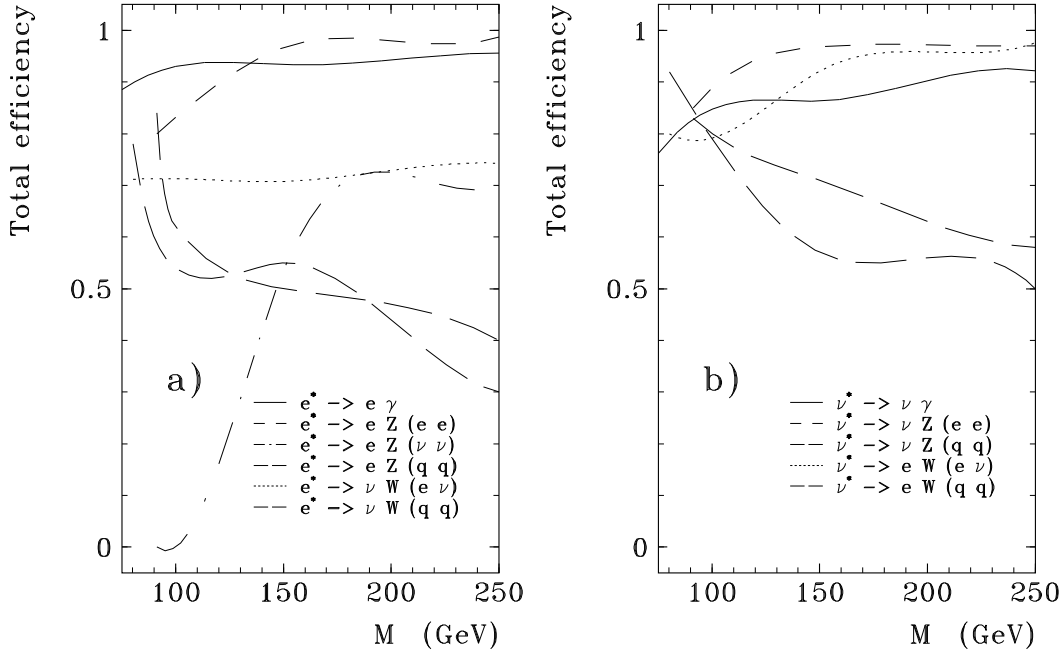


Figure 4: *Total detection efficiencies for specific decay channels of the excited leptons. In a) the efficiencies for detecting an excited electron and in b) the efficiencies for finding an excited neutrino are shown for the different final states investigated in this analysis.*

decay channels as functions of the mass of the excited states. The detection efficiency of the excited electron decreases rapidly for masses below 25 GeV. In principle coupling limits could be calculated up to the total centre of mass energy. However, in this analysis the calculations are limited to masses and coupling values where the decay width is well below the corresponding mass of the heavy lepton. For excited electrons and a special choice of the coupling $c_{\gamma e^* e}^2 = 1/16$ the total decay width is 28(210) GeV at $M = 225(250)$ GeV, taking into account the limits for Λ obtained from our analyses. If $c_{\gamma \nu^* \nu}^2 = 1/4$ is chosen, the width of the excited neutrino is 52(132) GeV for $M = 165(180)$ GeV.

The results improve the limits from earlier H1 detector data [5] by a factor of ≈ 4 in this newly accessible mass region. Searches for e^* and ν^* have been pursued at LEP mainly, using the decay channels with a photon in the final state. The current rejection limits for the direct single production of leptons exclude masses $\lesssim 90$ GeV, almost independently of the compositeness scale Λ for $\Lambda \leq 2.5$ TeV [19].

The best limits for e^* production in the HERA mass range are obtained in the $e\gamma$ final state due to the high detection efficiency. The sensitivity for the ν^* is suppressed by the W propagator as opposed to the photon propagator in the case of e^* production. For a typical value $c_{\gamma e^* e}^2 = 1/4$ and at a mass around 100 GeV, we currently rule out compositeness scale parameters $\Lambda \lesssim 300$ GeV. The rejection limits for final states with a W or Z boson are similar, the main difference occurring because of Z decays into $\nu\bar{\nu}$.

Finally, we would like to comment on Majorana neutrinos ν_M . At HERA, the production of ν_M with masses $m \gtrsim 100$ GeV and a mixing of 0.01 is possible and would give a cross section $\mathcal{O}(0.1 \text{ pb})$ at 100 GeV [20]. We have used models that predict these types of neutrinos and our detection efficiencies only change marginally compared to the excited lepton efficiencies. The data presented in this paper limits the accessible mixing to about 0.8. Only when the accumulated luminosity at HERA reaches $\mathcal{O}(50 \text{ pb}^{-1})$ will the HERA detectors be able to reduce the mixing limits significantly.

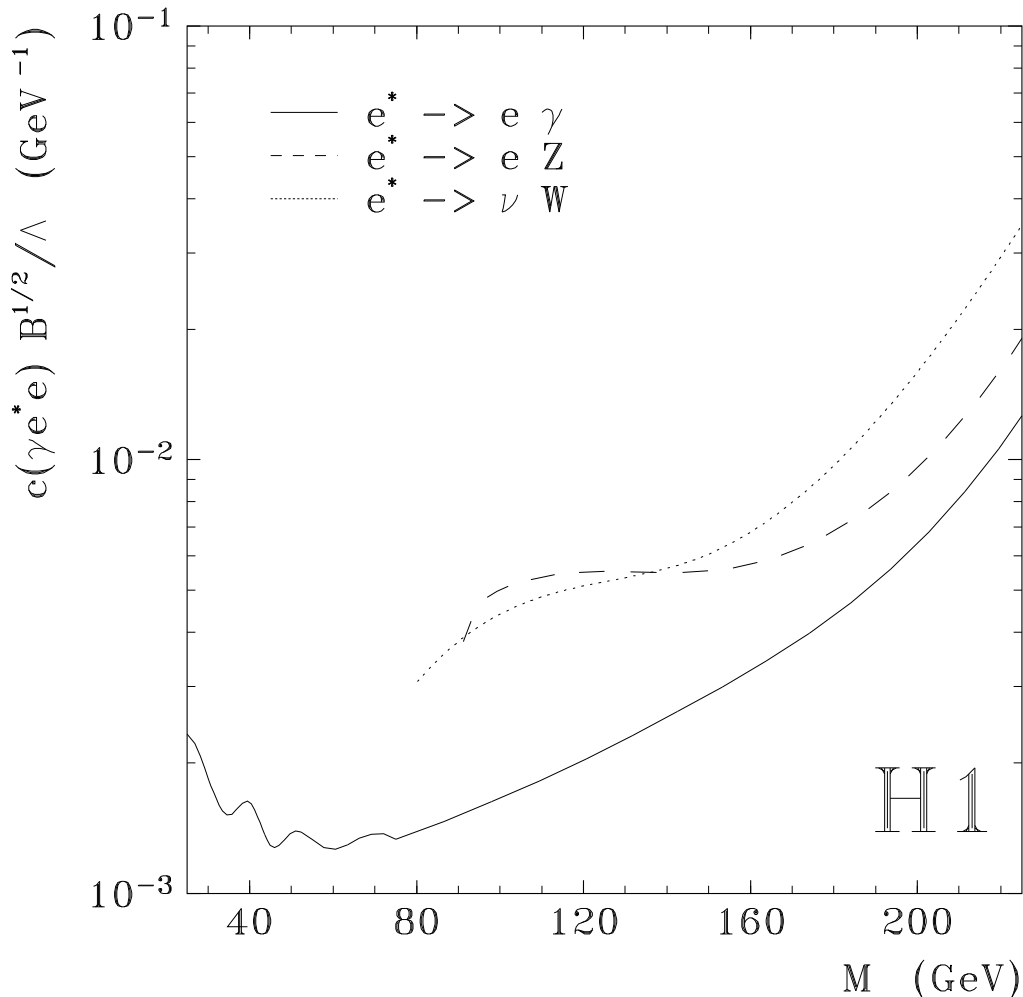


Figure 5: *Rejection limits with a CL of 95% for the e^* . Regions above the curves are excluded. In the channel $e^* \rightarrow e \gamma$ the WAB events have been used to calculate limits. For final states with jets the limits are derived using data set 2 with $E_{ti} > 15$ GeV, $i = 1, 2$ and then combined with the results from other decay modes of the Z and W.*

7 Conclusions

The H1 detector has been used to search for direct production of heavy leptons L in a mass range from 10 GeV up to 225 GeV. This mass range is directly accessible only at the ep collider HERA. The available centre of mass energy allows a mass range to be explored where L can decay into final states including W and Z bosons. Therefore the analyses presented here include an investigation of several final state topologies. No evidence was found for the production of heavy leptons. Cross sections above $\mathcal{O}(10)$ pb are ruled out with 95% CL, depending on the final state considered. For the direct search of the excited states e^* and ν^* , limits on couplings have been presented.

8 Acknowledgements

We are very grateful to the HERA machine group whose outstanding efforts made this experiment possible. We wish to acknowledge the support of the DESY technical staff. We appreciate the many contributions of our engineers and technicians who constructed and maintained the detector. We thank the funding agencies for financial support of this experiment. We also wish

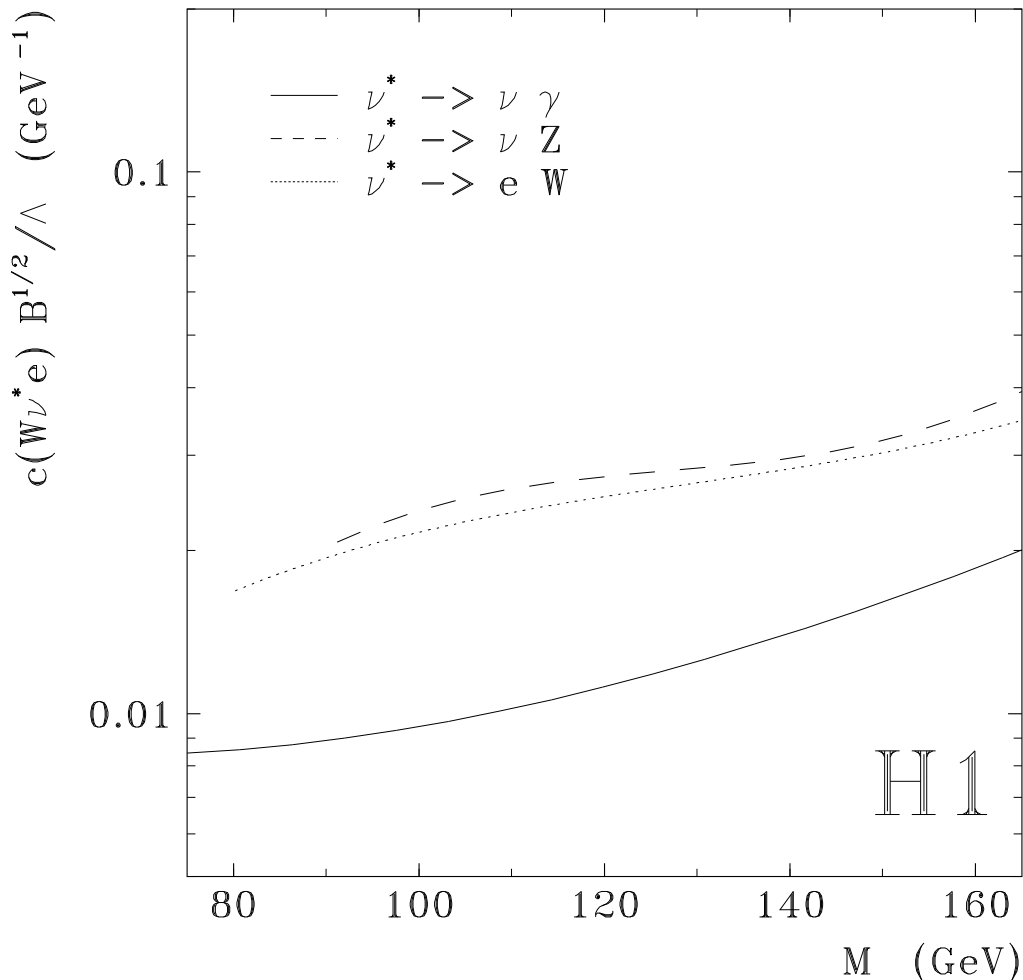


Figure 6: *Rejection limits with a CL of 95% for the ν^* . Regions above the curves are excluded. For final states with jets the limits are derived using data set 2 with $E_{t_i} > 15$ GeV, $i = 1, 2$ and then combined with the results from other decay modes of the Z and W.*

to thank the DESY directorate for the hospitality extended to the non-DESY members of the collaboration.

References

- [1] See, e.g.,
M.E. Peskin, Proc. of the Xth Symposium on Lepton-Photon Interactions, Ed. W. Pfeil, Bonn (1981) p. 880.
- [2] For a review, see P. Langacker, in Neutrinos, Ed. H.V. Klapdor (Springer, Berlin, 1988) p. 71.
- [3] W. Buchmüller and C. Greub, Nucl. Phys. B363 (1991) 345; W. Buchmüller et al., in proceedings Physics at HERA, Eds. W. Buchmüller, G. Ingelman, DESY Hamburg 1991, vol. 2, p. 1003.
- [4] F. Boudjema et al., in proceedings Physics at HERA, Eds. W. Buchmüller, G. Ingelman, DESY Hamburg 1991, vol. 2, p. 1094, and references therein.
- [5] I. Abt et al., H1 Collaboration, Nucl. Phys. B396 (1993) 3.
- [6] M. Derrick et al., Zeus Collaboration, Phys. Lett. B316 (1993) 207.

- [7] I. Abt et al., H1 Collaboration, The H1 detector at HERA, DESY preprint 93-103 (July 1993).
- [8] F. Raupach, in proceedings Physics at HERA, Eds. W. Buchmüller, G. Ingelman, DESY Hamburg 1991, vol. 3, p. 1473.
- [9] G. Ingelman, (LEPTO version 5.2), program manual unpublished; H. Bengtsson, G. Ingelman and T. Sjöstrand, Nucl. Phys. B301 (1988) 554.
- [10] J.E. Huth et al., FERMILAB-Conf-90/249-E (1990).
- [11] T. Sjöstrand, in proceedings Physics at HERA, Eds. W. Buchmüller, G. Ingelman, DESY Hamburg 1991, vol. 3, p. 1405, and references therein.
- [12] Bo Andersson, G. Gustafson and T. Sjöstrand, Phys. Lett. B94 (1980) 211; Bo Andersson et al., Phys. Rep. (1983) 31.
- [13] E. Theuer, in proceedings Physics at HERA, Eds. W. Buchmüller, G. Ingelman, DESY Hamburg 1991, vol. 3, p. 1497.
- [14] F.E. Low, Phys. Rev. Lett. 14 (1965) 238; N. Cabibbo, L. Maiani and Y. Srivastava, Phys. Lett. B 139 (1984) 459; J.H. Kühn and P. Zerwas, Phys. Lett. B 147 (1984) 189; F.M. Renard, Phys. Lett. B126 (1983) 59; A. De Rújula, L. Maiani and R. Petronzio, Phys. Lett. B140 (1984) 253.
- [15] K. Hagiwara, S. Komamiya and D. Zeppenfeld, Z. Phys. C29 (1985) 115.
- [16] F. Boudjema, A. Djouadi and J.L. Kneur, Z. Phys. C57 (1993) 425.
- [17] T. Köhler, in proceedings Physics at HERA, Eds. W. Buchmüller, G. Ingelman, DESY Hamburg 1991, vol. 3, p. 1526.
- [18] K. Hikasa et al., Particle Data Group, Phys. Rev. D45 (1992) part II; H. Mönch, PI-THA 91/2, thesis RWTH-Aachen (1991).
- [19] D. Decamp et al., ALEPH Collaboration, Phys. Rep. 216 (1992) 253; O. Adriani et al., L3 Collaboration, Phys. Lett. B288 (1992) 404; B. Adeva et al., L3 Collaboration, Phys. Lett. B252 (1990) 525; M.Z. Akrawy et al., OPAL Collaboration, Phys. Lett. B257 (1991) 531; Idem, Phys. Lett. B244 (1990) 135.
- [20] G. Ingelman, J. Rathsman, DESY preprint 93-039, Hamburg (March 1993) and preprint TSL/ISV-93-0081.